

# 얇은 셸 구조의 실시간 동적 탄성 변형

최민규\* 고흥석† 우승용‡<sup>o</sup>

\*‡광운대학교 †서울대학교

\*mgchoi@kw.ac.kr †ko@graphics.snu.ac.kr ‡sywoo@cs.kw.ac.kr

## Real-Time Elastodynamic Deformation of Thin Shell Structures

Min Gyu Choi\* Hyeong-Seok Ko† Seung Yong Woo‡<sup>o</sup>

\*‡Kwangwoon University †Seoul National University

### Abstract

This paper proposes a real-time simulation technique for thin shells undergoing large deformation. Thin shells are almost two-dimensional structures visually well approximated as surfaces, such as leaves, paper sheets, hats, aluminum cans. Unfortunately accurate simulation of these structures requires one of the most complex formulations in continuum mechanics, *shell theory* [4]. Moreover, there has not yet been any work reported to produce visually convincing animation of them while achieving real-time performance. Motivated by *discrete shells* [5] and *modal warping* [3], we formulate dynamics of thin shells using mass-spring models instead of finite element models, and then apply the modal warping technique to cope with large rotational deformation of thin shells. Experiments show that the proposed technique runs in real-time, and that it can simulate large bending and/or twisting deformations with acceptable realism.

## 1 Introduction

Thin shells are almost two-dimensional structures that can be interpreted as degenerate elastic solids and visually well approximated as surfaces, such as leaves, paper sheets, hats, aluminum cans (See Figure 1). They are known to be remarkably difficult to simulate because of their degeneracy in one dimension; Modeling thin shells as three-dimensional elastic solids requires very fine FEM [9] meshes to correctly capture the global bending behavior. On the other hand, accurate modeling and simulation of these structures with moderately-sized meshes requires one of the most complex formulations in continuum mechanics, *shell theory* [4]. Regardless of the approach, there has not yet been any method reported to produce visually convincing animation of thin shells while achieving real-time performance.

In this paper, we propose a real-time simulation technique for thin shells undergoing large rotational deformation. Motivated by *discrete shells* proposed by Grinspun et al.[5], we formulate dynamics of thin shells using mass-spring models instead of finite element models developed in shell theory. For real-time performance of simulation, we extend the modal warping technique, which was originally proposed by Choi and Ko [3] for large rotational deformation of elastic solids, to cope with thin shell structures. Experiments show that the proposed technique runs in real-time, and that it can simulate large bending and/or twisting deformation of thin shells with acceptable realism.

## 2 Dynamics of Thin Shell Structures

We use an arbitrary two-manifold triangle mesh to describe the shell geometry and model dynamics of thin shell structures using nonlinear energy functions for membrane and flexure that measure the differences between the undeformed and the deformed state of the triangle mesh, as proposed in [5]. The membrane energy is to model the elastic surfaces resisting on *intrinsic* deformations such as stretching (local changes in area) and shearing (local changes in length but not area). The flexural energy is for *extrinsic* deformations such as bending (local changes in curvature).

### 2.1 Membrane Energy

The membrane energy consists of the stretching and shearing energies. To measure the amount of stretch, we employ the triangle-based energy function that sums up the local changes in area over all the triangles:

$$E_A \triangleq \sum_A \frac{(\|A\| - \|\bar{A}\|)^2}{\|\bar{A}\|}, \quad (1)$$

where  $\|A\|$  and  $\|\bar{A}\|$  are the areas of the triangle  $A$  in the deformed and the rest state, respectively.

For the membrane energy that measures the amount of shear, we use the edge-based energy function that sums up the local



Figure 1: Leaves of a plant excited by rigid motion of the pot.

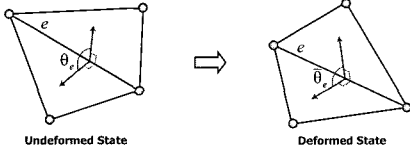


Figure 2: Dihedral angle of an edge for the flexural energy.

changes in length over all the edges:

$$E_L \triangleq \sum_L \frac{(\|e\| - \|\bar{e}\|)^2}{\|\bar{e}\|}, \quad (2)$$

where  $\|e\|$  and  $\|\bar{e}\|$  are the lengths of the edge  $e$  in the deformed and the rest state, respectively.

Then, we can represent the membrane energy of the shell as the sum of the energies for stretching and shearing:

$$E_M \triangleq k_A E_A + k_L E_L, \quad (3)$$

where  $k_A$  and  $k_L$  are the material constants for stretching and shearing, respectively.

## 2.2 Flexural Energy

To measure the flexural energy of the shell, we adopt the discrete flexural energy proposed by Grinspun et al. [5],

$$E_B \triangleq \sum_e 3 (\theta_e - \bar{\theta}_e)^2 \frac{\|\bar{e}\|}{h_e}, \quad (4)$$

where  $\theta_e$  and  $\bar{\theta}_e$  are the dihedral angles of the edge  $e$  measured in the deformed and the rest state, respectively, and  $h_e$  is the average of the heights of the two triangles sharing the edge  $e$  in the rest state (See Figure 2). This energy function was obtained by integrating the squared difference of mean curvature at a point over the piecewise linear mesh of the shell, and then by discretizing the integral (See [5] for the detailed derivation).

## 2.3 Governing Equation

The total elastic energy of a thin shell is then defined by the sum of the membrane and flexural energies:

$$E \triangleq E_M + k_B E_B, \quad (5)$$

where  $k_B$  is the bending or flexural stiffness constant.

By differentiating the above energy function with respect to the displacements of the mesh nodes, we can obtain the generalized elastic force due to the elastic potential energy of a thin shell,

$$\mathbf{f}(\mathbf{u}) = \frac{\partial E(\mathbf{u})}{\partial \mathbf{u}}, \quad (6)$$

where  $\mathbf{u}(t)$  is a  $3n$ -dimensional vector that represents the displacements of the  $n$  nodes from their original positions. Note that the elastic force vector  $\mathbf{f}$  must be zero when the displacement vector  $\mathbf{u}$  is zero. Thus, the elastic force can also be represented by  $\mathbf{f}(\mathbf{u}) = \mathbf{K}(\mathbf{u})\mathbf{u}$ .

Then, the governing equation for the thin shell structure can be written as

$$\mathbf{M}\ddot{\mathbf{u}} + \mathbf{C}\dot{\mathbf{u}} + \mathbf{K}(\mathbf{u})\mathbf{u} = \mathbf{F}, \quad (7)$$

where  $\mathbf{M}$  and  $\mathbf{C}$  are the constant mass and damping matrices, respectively, and  $\mathbf{F}(t)$  is a  $3n$ -dimensional vector that represents the external forces acting on the  $n$  nodes. Here, the elastic force term  $\mathbf{K}(\mathbf{u})\mathbf{u}$  is nonlinear with respect to  $\mathbf{u}$ , and thus the governing equation of the form (7) could not yet be integrated in real-time.

## 3 Simulation with Modal Warping

For real-time simulation of thin shells, we are to utilize the modal warping technique [3], which was proposed originally to extend modal analysis to cope with large rotational deformation of elastic solids. Through the use of the modal warping technique, a system of nonlinear equations of the form (7) can be approximated by a decoupled system of ordinary differential equations (ODEs), only a small number of which are sufficient for visually plausible simulation and also able to be independently integrated in real-time.

### 3.1 Modal Warping

The key idea of the modal warping technique is applying modal analysis to a equation of the form (7) in the local coordinate frames attached to the mesh nodes, in order to obtain the form shown in Equation (10). Let  $\mathbf{R}$  be the  $3 \times 3$  block-diagonal matrix, of which  $i$ -th block is the rotation matrix representing the orientation of the local coordinate frame attached to the  $i$ -th node. Then, premultiplying  $\mathbf{R}$  to both sides of Equation (7) and making assumptions on *commutativity in fine meshes* and *warped stiffness* [3] result in

$$\mathbf{M}\ddot{\mathbf{u}}^L + \mathbf{C}\dot{\mathbf{u}}^L + \mathbf{K}\mathbf{u}^L = \mathbf{R}^T \mathbf{F}, \quad (8)$$

where  $\mathbf{K}$  is  $\mathbf{K}(\mathbf{u})$  in the rest state, that is,  $\frac{\partial \mathbf{f}}{\partial \mathbf{u}}|_0$ , and  $\mathbf{u}^L$  is the generalized displacement vector measured and accumulated in the time-varying local coordinate frames.

In general,  $\mathbf{M}$  and  $\mathbf{K}$  are not diagonal, and thus Equation (8) is a coupled system of ODEs. Let  $\Phi$  and  $\Lambda$  be the solution matrices of the generalized eigenvalue problem,  $\mathbf{K}\Phi = \mathbf{M}\Phi\Lambda$ , such that  $\Phi^T \mathbf{M} \Phi = \mathbf{I}$  and  $\Phi^T \mathbf{K} \Phi = \Lambda$ . Since the columns of  $\Phi$  form

a basis of the  $3n$ -dimensional space,  $\mathbf{u}^L$  can be expressed as a linear combination of the columns:

$$\mathbf{u}^L(t) = \Phi \mathbf{q}(t). \quad (9)$$

Here,  $\Phi$  is the *modal displacement matrix*, of which the  $i$ -th column represents the  $i$ -th mode shape, and  $\mathbf{q}(t)$  is a vector containing the corresponding modal amplitudes as its components. By examining the eigenvalues we can take only the  $m$  dominant columns of  $\Phi$ , significantly reducing the amount of computation.

Substitution of Equation (9) into Equation (8) followed by a premultiplication of  $\Phi^T$  decouples Equation (8) as

$$\mathbf{M}_q \ddot{\mathbf{q}} + \mathbf{C}_q \dot{\mathbf{q}} + \mathbf{K}_q \mathbf{q} = \Phi^T (\mathbf{R}^T \mathbf{F}). \quad (10)$$

where  $\mathbf{M}_q = \mathbf{I}$ ,  $\mathbf{C}_q = (\xi \mathbf{I} + \zeta \Lambda)$ , and  $\mathbf{K}_q = \Lambda$  are now all diagonal<sup>1</sup>, and  $\Phi^T (\mathbf{R}^T \mathbf{F})$  is the modal force in the local coordinate frames. The above decoupled ODEs can be solved numerically for  $\mathbf{q}^k$  at the  $k$ -th time step using the Newmark integration scheme [8], and the corresponding displacement vector  $\mathbf{u}^k$  can be computed analytically:

$$\mathbf{u}^k = \int_0^{t^k} \mathbf{R}(t) \dot{\mathbf{u}}^L(t) dt = \tilde{\mathbf{R}}^k \Phi \mathbf{q}^k, \quad (11)$$

where the  $3 \times 3$  block-diagonal matrix  $\tilde{\mathbf{R}}^k$  is involved with only  $\mathbf{R}^k$  and  $\mathbf{q}^k$  [3].

### 3.2 Modal Rotation

For real-time simulation of thin shells, we now only need to develop an efficient way of tracking the local coordinate frames attached to the mesh nodes. Let  $\mathbf{w}_A$  be the rotation vector of a triangle  $A$  that rotates the local coordinate frame attached to the triangle  $A$  in the undeformed state by the angle  $\theta = \|\mathbf{w}_A\|$  about the unit axis  $\hat{\mathbf{w}}_A = \mathbf{w}_A / \|\mathbf{w}_A\|$ . This rotation vector must be a purely geometric function of the displacements of the three triangle nodes,  $\mathbf{u}_A = [\mathbf{u}_{(A,1)}^T | \mathbf{u}_{(A,2)}^T | \mathbf{u}_{(A,3)}^T]$ . Then, we can expand  $\mathbf{w}_A(\mathbf{u}_A)$  near the undeformed state by

$$\mathbf{w}_A(\mathbf{u}_A) = \mathbf{w}_A(\mathbf{0}) + \left. \frac{\partial \mathbf{w}_A}{\partial \mathbf{u}_A} \right|_{\mathbf{0}} \mathbf{u}_A + O(\mathbf{u}_A^2), \quad (12)$$

where  $\partial \mathbf{w}_A / \partial \mathbf{u}_A$  is the  $3 \times 9$  Jacobian matrix evaluated at the undeformed state. Here  $\mathbf{w}_A(\mathbf{0})$  is the zero vector because there is no rotation at the undeformed state. For the rotation vector of a node, we use the average of the rotation vectors of all the triangles sharing the node.

Based on the above discussion, we can now assemble  $\mathbf{W}_A$  of all the triangles to form the global matrix  $\mathbf{W}$  such that  $\mathbf{W}\mathbf{u}$  gives the composite vector  $\mathbf{w}$ , which is concatenation of all the three-dimensional rotation vectors of the mesh nodes. When assembling  $\mathbf{W}$ ,  $3 \times 3$  submatrices of  $\mathbf{W}_A$  for the rotation vectors of

<sup>1</sup>Here, we took the commonly adopted assumption (*Rayleigh damping*) that  $\mathbf{C} = \xi \mathbf{M} + \zeta \mathbf{K}$ , where  $\xi$  and  $\zeta$  are scalar weighting factors.

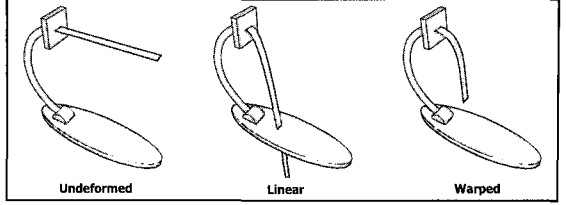


Figure 3: A flat beam (left) is deformed by linear modal analysis (middle) and by modal warping (right). Linearization artifacts are not observed in the modal warping case.

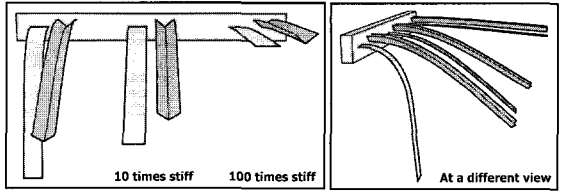


Figure 4: Three pairs of flat and v-beams with fixed stretching and shearing stiffness constants and increasing flexural stiffness constants (left to right).

all the triangles sharing a node are not summed up but averaged. Finally, expanding  $\mathbf{u}(t)$  with Equation (9) gives<sup>2</sup>

$$\mathbf{w}(t) \approx \mathbf{W} \Phi \mathbf{q}(t) \triangleq \Psi \mathbf{q}(t). \quad (13)$$

Both  $\mathbf{W}$  and  $\Phi$  are characterized by the thin shell at the rest state and are thus constant over time. Therefore we can precompute  $\Psi$ . The above equation shows that, as in the displacement (9), we can represent local rotations of mesh nodes in terms of  $\mathbf{q}(t)$ , which can also be computed in real-time. We call  $\Psi$  the *modal rotation matrix*.

## 4 Experiments

Our simulation scheme was implemented as an Alias MAYA plugin for a Microsoft Windows<sup>xp</sup> environment. To obtain the  $m$  dominant eigenvalues of large sparse square matrices and the corresponding eigenvectors, we used the built-in C++ math function `eigs` in MATLAB. All experiments were performed on a PC with an Intel Pentium D 3.46GHz processor, 2GB memory, and an nVIDIA GeForce FX 7900 GTX graphics card. We used the time step size of  $h = 1/30$  second in all experiments reported in this section, and the simulation ran in real-time.

The first experiment is to compare the results generated by traditional linear modal analysis [7] and modal warping for thin shells. We simulated the deformation of a flat beam under a gravitational field using the two methods. It is clear from the simulation results shown in Figure 3 that linearization in modal analysis

<sup>2</sup>We are considering the rest state, so  $\mathbf{u}(t)$  can be interpreted as  $\mathbf{u}^L(t)$ .

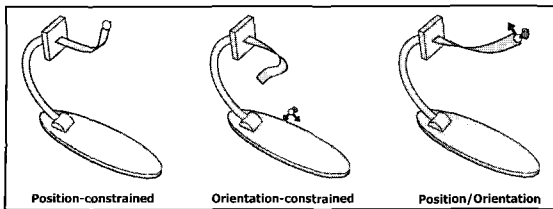


Figure 5: A flat beam manipulated with position (left), orientation (middle), and position/orientation constraints (right). The position constraints are represented by yellow spheres and the orientation are represented by RGB axes.

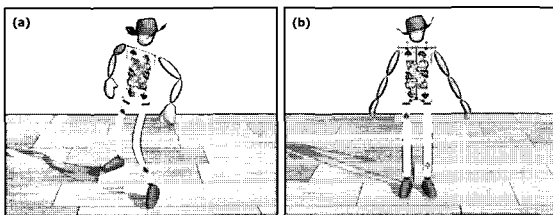


Figure 6: Constraint-driven animation of a character consisting of four deformable sheets (the hat, body, and both legs).

leads to artifacts that are not observed in the case of modal warping for thin shells.

The next experiment is to demonstrate the effect of varying flexural stiffness in a high dynamic range. Figure 4 shows, from left to right, a pair of flat and v-beam with increasing flexural stiffness constants. In all cases, simulation was numerically stable and the results were visually convincing. Although the material properties of the v-beam are the same with those of the flat beam, the non-flat cross section of the v-beam contributes to making the structural rigidity more stiff, especially for low flexural stiffness, as pointed out in [5].

The manipulation constraints introduced in modal warping for elastic solids [3] can also be applied to modal warping for thin shells. Figure 5 demonstrates the manipulation capability for thin shells. From left to right, the resultant deformations are in the cases of (1) only position constraints, (2) only orientation constraints, and (3) both position and orientation constraints.

Furthermore, the manipulation constraints can be used to animate a thin-shelled deformable character. We simulated a character whose upper body, and both legs are deformable sheets (Figure 6a). As the character made a dance motion, the deformable sheets made a dynamic passive deformation, excited by the gross body motion of the character. The positions of all the mesh nodes contained in the red cylinders and spheres at the initial setup were statically constrained. As shown in Figure 6b, the deformable sheets are attached to the skeleton by position/orientation constraints (the RGB axes).

## 5 Conclusion

In this paper, we proposed a real-time simulation technique for thin shells that can be visually well approximated as two-dimensional surfaces, such as leaves, paper sheets, hats, aluminium cans. We formulated dynamics of thin shells using mass-spring models [5] instead of finite element models [6] so as to make the technique easy to understand and, more importantly, easy to implement. Then, we extended the modal warping technique, which was originally proposed for elastic solids [3], so as to accommodate large rotational deformation of thin shells while achieving real-time performance. Furthermore, we incorporated the manipulation constraints introduced originally for elastic solids; The constraints can be used for some less obvious but very useful purposes, such as to model a thin-shelled deformable character as demonstrated in the experiments.

An interesting feature of our technique is that it does not assume specific energy functions a priori, although the current implementation employs the energy functions proposed in [5]. As a consequence, it can be thought of as a general framework not as a specific scheme. One can employ other energy functions used for traditional cloth simulation [2, 1]. We expect the proposed technique will prove useful in many application areas, including computer games and character animation.

## Acknowledgment

This work was supported in part by Seoul Research and Business Development Program (10581), Ministry of Information and Communication under the Information Technology Research Center (ITRC) support program, Ministry of Science and Technology under National Research Laboratory (NRL) grant M10600000232-06J0000-23210, Ministry of Information and Communication, the Brain Korea 21 Project, and Automation and Systems Research Institute at Seoul National University.

## References

- [1] D. Baraff and A. Witkin. Large steps in cloth simulation. *Computer Graphics (Proc. ACM SIGGRAPH '98)*, 32:43–54, 1998.
- [2] R. Bridson, S. Marino, and R. Fedkiw. Simulation of clothing with folds and wrinkles. In *Proc. ACM SIGGRAPH/Eurographics Symp. Computer Animation*, pages 28–36, 2003.
- [3] M. G. Choi and H.-S. Ko. Modal warping: Real-time simulation of large rotational deformation and manipulation. *IEEE Transactions on Visualization and Computer Graphics*, 1(1):91–101, 2005.
- [4] A. E. Green and W. Zerna. *Theoretical Elasticity*. Oxford University, 1968.

- [5] E. Grinspun, A. N. Hirani, M. Desbrun, and P. Schröder. Discrete shells. In *Proc. ACM SIGGRAPH/Eurographics Symp. Computer Animation*, pages 49–54, 2003.
- [6] E. Grinspun, P. Krysl, and P. Schröder. CHARMS: A simple framework for adaptive simulation. *ACM Transactions on Graphics (Proc. ACM SIGGRAPH 2002)*, 21(3):281–290, 2002.
- [7] K. K. Hauser, C. Shen, and J. F. O’Brien. Interactive deformation using modal analysis with constraints. In *Proc. Graphics Interface*, pages 247–255, 2003.
- [8] N. M. Newmark. A method of computation for structural dynamics. *ASCE Journal of the Engineering Mechanics Division*, 85(3):67–94, 1959.
- [9] O. C. Zienkiewicz. *The Finite Element Method*. McGraw-Hill Book Company (UK) Limited, Maidenhead, Berkshire, England, 1977.